Basilar skull fracture in a Thoroughbred colt: Radiography or computed tomography?

Authors:
Chee Kin Lim[1]
Montague N. Saulez[1]
Adrienne Viljoen[1]
Ann Carstens[1]

Affiliations:
[1]Department of Companion Animal Clinical Studies, University of Pretoria, South Africa

Correspondence to:
Chee Kin Lim

Email:
cklimvet@yahoo.com

Postal address:
Private Bag X04, Onderstepoort 0110, South Africa

Dates:
Received: 28 May 2012
Accepted: 12 Jan. 2013
Published: 19 Apr. 2013

How to cite this article:
Lim, C.K., Saulez, M.N., Viljoen, A. & Carstens, A., 2013, 'Basilar skull fracture in a Thoroughbred colt: Radiography or computed tomography?', *Journal of the South African Veterinary Association* 84(1), Art. #251, 6 pages. http://dx.doi.org/10.4102/jsava.v84i1.251

A two-year-old Thoroughbred colt was presented to the Equine Clinic, Onderstepoort Veterinary Academic Hospital for head trauma after rearing and falling backwards, hitting his head on the ground. Following medical therapy for acute onset neurological impairment secondary to a suspected basilar skull fracture, the horse was anaesthetised and computed tomography of the skull was performed. A diagnosis of a comminuted basilar skull fracture was made and skull radiographs were taken for comparison. The horse was subsequently euthanased owing to the poor prognosis; necropsy findings were compatible with imaging findings. The value and limitation of computed tomography versus radiography for the diagnosis of basilar skull fracture are discussed in this report.

Introduction

Falling over backwards is the single most common event that leads to basilar skull fracture in horses (Ragle 1993). Although head trauma can occur at any age, young horses are particularly prone to head injury as they are more likely to resist restraint of the head than older horses. The basilar part of the skull consists of the presphenoid, basisphenoid and basioccipital bones. The body of the basisphenoid bone articulates caudally with the rostral aspect of the basioccipital bone and this suture line can be seen radiographically up to five years of age (Butler *et al.* 2008). In a clinically normal horse, this line can be as much as three times wider ventrally than dorsally (Ackerman, Coffman & Corley 1974). Basisphenoid–basioccipital bone fractures are often associated with avulsion fractures at the insertion of the flexor muscles at the base of the skull (e.g. rectus capitis ventralis major, rectus capitis ventralis minor and longus capitis ventralis) (Feary *et al.* 2007; McSloy *et al.* 2007; Ragle 1993; Ramirez III, Jorgensen & Thrall 1998) and are associated with high morbidity and mortality (McSloy *et al.* 2007; Ragle 1993). The six typical radiographic findings suggestive of equine basilar skull fractures are displacement of the basisphenoid–basioccipital suture line, soft tissue opacification of the Eustachian tube diverticula (ETD), ventral deviation of the dorsal pharyngeal wall, attenuation of the nasopharynx, bony fragments in the ETD and the presence of gas opacities in the cranial vault or cranial cervical spine (Ramirez III *et al.* 1998). However, radiographic diagnosis of basilar skull fractures can be challenging, particularly when displacement of the fracture fragment is minimal.

Computed tomography (CT) has been widely acknowledged to be superior to conventional radiography in the diagnosis of basilar skull fractures owing to its ability to produce a tomographic slice that eliminates superimposition of overlying bony and soft tissue structures (Avella & Perkins 2011; Beccati *et al.* 2011; McSloy *et al.* 2007). In addition, the ability to reconstruct multiplanar reformatted images in dorsal, sagittal or oblique imaging planes provides invaluable pre-operative information for surgical planning (Kinns & Pease 2009). The normal CT anatomy of the equine head is well described (Morrow *et al.* 2000; Solano & Brawer 2004).

This case report compares the advantages and disadvantages of CT and radiography when dealing with basilar skull fractures in a horse.

Case history and imaging findings

A two-year-old Thoroughbred colt, approximately 475 kg, fell over backwards in a horsebox during loading. After being unconscious for four hours, the colt was referred to the Onderstepoort Veterinary Academic Hospital the next day. On admission, the colt was conscious, in sternal recumbency and tachycardic (52 beats per minute). There was fresh blood present at both left and right external ear openings, as well as at the right nostril. Following repeated, uncontrollable attempts to stand, the colt was sedated intravenously with 20 mg romifidine (Sedivet®, Boehringer Ingelheim, South Africa) and 1500 mg hydrocortisone sodium succinate (Solu-cortef™, Pfizer, South Africa). Direct and indirect pupillary light response was present bilaterally. A complete neurological examination could not be performed owing to the animal's further repeated efforts

to stand, and restricted access and safety concerns in the horse trailer. Following intravenous (IV) catheterisation, benzylpenicillin at 22 000 IU/kg (Fresenius Kabi, Bodene, South Africa) and gentamicin sulphate at 6.6 mg/kg (Genta 50, Phenix SA, South Africa) were administered for antimicrobial coverage. The bladder was catheterised prior to induction of general anaesthesia (GA). A total of 1.2 L hypertonic saline (NaCl 5%, Fresenius Kabi, Bodene, South Africa) was administered intravenously to reduce intracranial pressure, followed by 12 L polyionic crystalloid fluid (Sabax Plasma Vet, Adcock Ingram, South Africa). Basilar skull fractures with subdural haemorrhage were suspected and CT of the skull was performed.

The colt was premedicated with diazepam 50 mg IV (Pox®, Pharmacies, South Africa), induced with thiopentone 6 g IV (Bomathal™, Merial, South Africa) and maintained on isoflurane (Isofor®, Safeline Pharmaceutical [Pty] Ltd., South Africa) at a 3% concentration and oxygen flow rate of 6 L/min. A CT scan was performed using a fourth-generation Siemens Emotion Duo CT system (Siemens Medical Systems, Forchheim, Germany) with a sliding gantry and viewed in bone, spine and cerebrum windows. The scan parameters were 110 kV and 11 mA, with a pitch of 2 and slice thickness of 3 mm. The field of view extended from the cranial third of the second cervical vertebra to the last molar, with the animal positioned in dorsal recumbency.

CT findings revealed severe bilateral comminuted fractures of the basisphenoid–basioccipital physeal junction (Figure 1). There were also small, multifocal, hypoattenuating gas bubbles and streaks (Hounsfield unit [HU] between –250 and –310) dissecting into the partially ruptured right rectus capitis muscle. Some of the gas was trapped between this muscle and the fracture fragments (Figure 2a). Asymmetric hypoattenuating areas around the brainstem and cranial spinal cord segment mimicking free gas in the subarachnoid space were considered to be epidural fat with the HU between –65 and –111 (Figures 2b and 2c). No intracranial or ETD haemorrhage was detected.

To compare the findings between CT and radiography, radiographs of the skull were taken immediately after the CT scan, under the same GA, using a ceiling-mounted Apelem Magnum 80 radiography machine (Medical Technology s.l.r., Italy) with a film focal distance of 100 cm. Left to right lateral, right ventral left dorsal oblique, left ventral right dorsal oblique and ventrodorsal views of the base of the skull were taken using 354 mm × 430 mm Fujifilm FCR IP Type CC cassettes (Fuji Photo Film, Japan). Films were processed with Fujifilm FCR Profect CS processor (Fujifilm, Japan). No grid was used. The radiographic images were viewed on a primary imaging work station with 2Mp monochrome medical grade monitors using software with digital imaging and communications in medicine (DICOM) capabilities.

On the lateral view, a 15 mm × 15 mm triangular to wedge-shaped fracture fragment was seen at the extreme caudal right aspect of the basisphenoid bone, with mild caudoventral displacement of the fracture fragment that formed a 5 mm step just at the ventral juncture of the basisphenoid–basioccipital suture line (Figure 3). In addition, the lateral view also showed a non-displaced, smaller triangular fracture fragment of approximately 10 mm × 4 mm at the extreme rostroventral aspect of the basioccipital bone (Figure 3). On the oblique views, these fracture fragments were characterised by an irregular ventral margin of the basisphenoid–basioccipital junction, but the outlines of the fracture fragments were difficult to visualise owing to superimposition of bony and soft tissue structures over the dorsal pharynx. On the ventrodorsal view, a 14 mm × 5 mm semilunar-shaped radiolucent fracture bed was noted on the right paramidline of the extreme caudal aspect of the basisphenoid bone, with mild right lateral displacement of the basisphenoid fracture fragment (Figure 4). All fracture edges were relatively blurred. No obliteration of the ETD or thickening of the dorsopharyngeal wall was noted.

Owing to the apparent instability of the extensive basilar skull fractures, a poor prognosis was given for recovery and return to racing. Euthanasia was recommended as the neurological impairment was unlikely to improve. Post-mortem findings were compatible with CT findings; severe comminuted fractures of the basisphenoid–basioccipital suture line were seen, but no intracranial haemorrhage was noted.

Discussion

Although CT has been acknowledged as the most ideal imaging modality for accurate diagnosis of basilar skull fractures (Beccati *et al.* 2011; McSloy *et al.* 2007; Ramirez III *et al.* 1998), the lack of direct access to this imaging modality in most local equine hospitals means that radiography is still a convenient and extremely useful diagnostic tool for quick detection of basilar skull fractures.

Contrary to reports that radiographic examination of the cranial vault is often unrewarding owing to superimposition of complex anatomic head structures (Beccati *et al.* 2011; Kinns & Pease 2009), we found that careful and detailed assessment of well-positioned, good-quality radiographs of the skull, to look specifically for typical radiographic findings of basilar skull fracture (Ramirez III *et al.*1998), certainly proved to be helpful in the identification of the basilar skull fractures in this case. The enhanced visibility of the basilar fracture fragments may also have been due partly to the ability to manipulate the brightness and contrast of the computed radiography images using computer software. Our findings agreed with a previous study (Ramirez III *et al.* 1998), which showed that the lateral radiographic view is most useful in identification of basilar fractures, particularly when looking for the step or displacement of the basisphenoid–basioccipital suture line. A good ventrodorsal or dorsoventral view, as shown in this case, aids in the detection of basilar skull fractures. Interpretation of the oblique views, however, is more likely to be hampered by superimposition of anatomic structures in

the dorsal pharyngeal region. The aforementioned findings are of particular significance, as both lateral and ventrodorsal views can be obtained with the horse standing. This means that in a horse with suspected cranial trauma, the animal need not be subjected to unnecessary GA for CT evaluation, which may incur more unwanted problems during post-GA recovery.

Radiographic diagnosis of basilar skull fractures can be challenging when there is no displaced bone fragment (Beccati *et al.* 2011; Feige *et al.* 2000; McSloy *et al.* 2007; Ramirez III *et al.* 1998). The limitation of skull radiography in demonstrating the severity of basilar skull fractures adequately was typically highlighted in this case, as the extent of the severity of the bilateral comminuted fracture

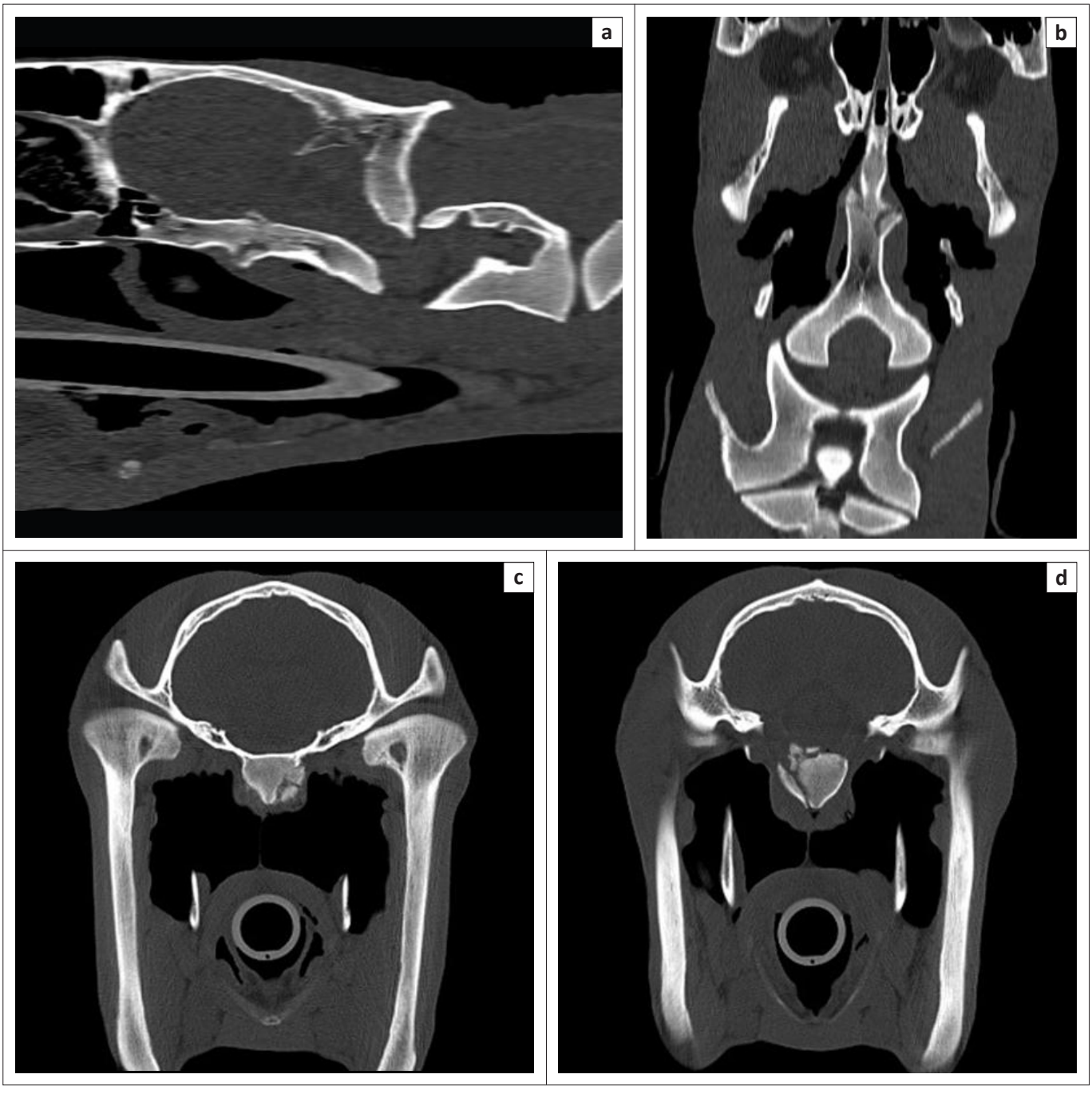

Window level 450; window width 1500.
Computed tomography parameters: 110 kV, 11 mA, 3-mm slice thickness, pitch 2.
An endotracheal tube is present in all images.
(a) Rostral is to the left of the image and dorsal is to the top of the image; (b) rostral is to the top of the image and right is to the left of the image; (c) and (d) right is to the left of the image.

FIGURE 1: Computed tomography images of the skull in bone window. (a) Midline sagittal slice of the head showing moderate ventral displacement of the caudoventral basisphenoid fracture fragment and an additional small fracture fragment from the rostrodorsal basioccipital bone. (b) Dorsal slice showing an irregular, long, incomplete fracture line in a right rostrolateral to left caudolateral orientation across the basisphenoid–basioccipital suture line, with a minimally displaced caudal basisphenoid fracture fragment at the right rostral aspect of the fracture line and a moderately displaced wedge-shaped rostral basioccipital fracture fragment at the left caudal aspect of the fracture line. (c) and (d) Transverse slices at the level of the basisphenoid–basioccipital physeal junction. A bilateral comminuted fracture of the left ventrolateral aspect of the caudal basisphenoid bone and right lateral and right dorsolateral aspect of the rostral basioccipital bone is noticeable. Normal, air-filled Eustachian tube diverticula can be seen.

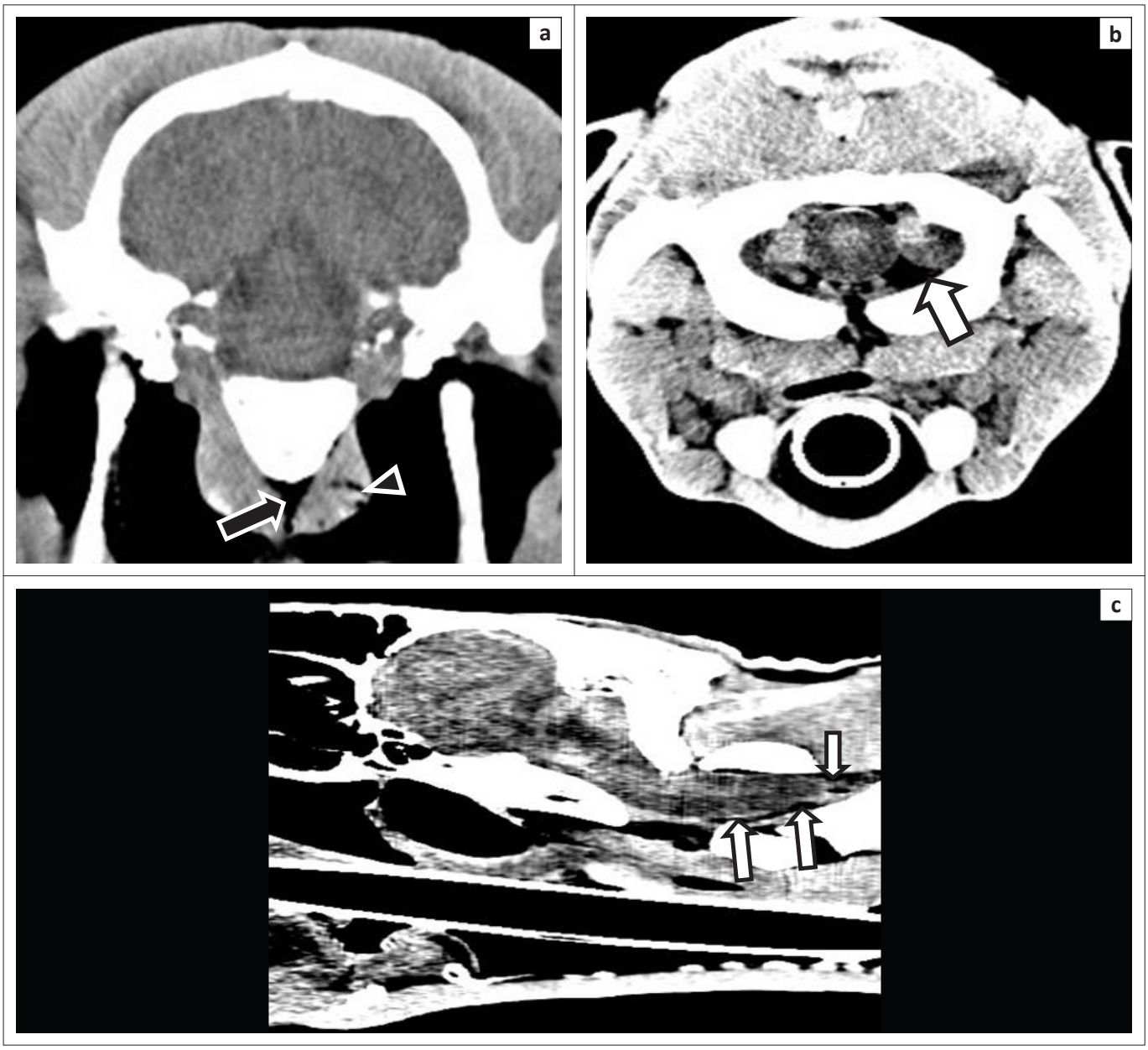

Spine window: Window level 40; window width 120.
Cerebrum window: Window level 35; window width 80.
Computed tomography parameters: 110 kV, 11 mA, 3 mm slice thickness, pitch 2.
(a) Right is to the left of the image and dorsal is to the top of the image; (b) right is to the left of the image and dorsal is to the top of the image; (c) rostral is to the left of the image and dorsal is to the top of the image.

FIGURE 2: Computed tomography images of the skull in spine window and cerebrum window. (a) Transverse slice at the level of the brainstem using the spine window. Small hypoattenuating gas bubbles and streaks (HU –250 to –310) can be seen dissecting into the partially ruptured left rectus capitis muscle (small black arrowhead), with a small amount of gas trapped between the muscle and the basisphenoid bone (black solid arrow). (b) Transverse slice at the level of the foramen magnum using the cerebrum window. A moderate amount of hypoattenuating epidural fat (HU –65 to –111) (solid white arrow) is seen around the spinal cord. (c) Parasagittal slice using the cerebrum window. A moderate amount of hypoattenuating epidural fat (HU –92) is seen around the cranial cervical cord region and slightly less so at the ventral brainstem region, mimicking 'pseudo' subarachnoid gas (solid white arrows).

of the basisphenoid–basioccipital physeal junction was not reflected as well as by CT. Radiography does not provide further information on possible intracranial damage such as intracranial haemorrhage, although there has been an isolated report of intracranial gas being seen radiographically following cranial trauma (Taylor *et al.* 1993).

CT provided not only a more accurate assessment of the severity of the basilar skull fracture with regard to the location, extent, configuration and number of fracture fragments but also a reasonable insight into possible intracranial pathology such as haemorrhage or gas, which can be extremely important for pre-operative surgical planning. The epidural fat around the spinal cord may mimic a 'pseudo' subarachnoid gas appearance owing to the narrow window width in spine and cerebrum windows. The normal HU for equine epidural fat has not been established but in small animals and humans, the epidural fat has a HU of –100 and between –80 and –120, respectively (Fiirgaard & Madsen 1997; Seiler *et al.* 2011). Determination of the HU is therefore of paramount importance to prevent misdiagnosis of subarachnoid gas accumulation. The ability of CT to

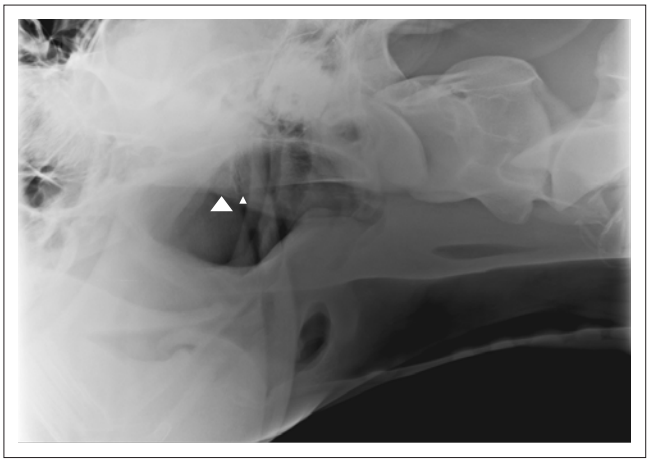

Settings: 90 kV, 2.5 mAs; no grid.
Rostral is to the left of the image and dorsal is to the top of the image.

FIGURE 3: Left-to-right lateral view of the skull centred on the basilar skull region. A well-marginated triangular fracture fragment (big arrowhead) at the most caudal aspect of the basisphenoid bone is visible with a 5 mm 'step' just at the ventral juncture of the basisphenoid–basioccipital suture line. In addition, a non-displaced smaller triangular fracture fragment (small arrowhead) can also be seen at the most rostroventral aspect of the basioccipital bone. Small amounts of gas are visible in the cranial oesophagus and a moderate amount of gas in the lateral laryngeal ventricles.

Settings: 90 kV, 5.6 mAs; no grid.
Right is to the left of the image and rostral is to the bottom of the image.

FIGURE 4: Ventrodorsal view of the skull centred on the basilar skull region. A semilunar-shaped radiolucent fracture bed (arrowhead) is seen on the right paramidline of the most caudal aspect of the basisphenoid bone, with mild right lateral displacement of the basisphenoid fracture fragment. The fracture edge appears slightly blurry.

provide cross-sectional slices allows further visualisation of possible rupture of the capital flexor muscles and assessment of the integrity of the medial wall of the ETD (Avella & Perkins 2011). Accurate assessment of the severity and location of intracranial and extracranial damage associated with basilar skull fractures is vital in providing a legitimate prognosis for survival or return to athletic function. Although the use of contrast medium allows detection of blood-brain barrier breakdown, recent studies have found that contrast-enhanced CT did not offer advantages over unenhanced CT when assessing equine intracranial pathologies (Lacombe, Sogaro-Robinson & Reed 2010; Sogaro-Robinson *et al.* 2009), largely because the effective IV dose of contrast medium for such studies has not been established yet. In addition, blood pressure and the state of recumbency of the patient may also play a role in limiting the availability and distribution of the contrast medium (Pollard, Pulchalski & Pascoe 2008; Sogaro-Robinson *et al.* 2009).

Although CT can provide rapid and accurate assessment of basilar skull fractures compared with radiography, the added risk arising from GA and recovery is a common reason for clinicians hesitating to opt for this imaging modality. Head trauma and central neurological signs in horses are often associated with poor recovery and survival after GA (Avella & Perkins 2011). However, the recent development of standing CT for the equine head negates the requirement of GA and offers an opportunity to make ante-mortem diagnosis of intracranial diseases (Jose-Cunilleras & Piercy 2007), but this may not be feasible in the neurologically compromised patient with basilar skull fractures. The added cost of CT is justified when the additional findings enable the clinician to decide on a specific surgical intervention, medical management or to provide advice for euthanasia if the prognosis is grave.

Conclusion

CT is superior to radiography in detecting and defining the severity of intracranial lesions (Avella & Perkins 2011; Beccati *et al.* 2011; McSloy *et al.* 2007; Ragle *et al.* 1988; Ramirez III *et al.* 1998). However, equine skull radiography may still be unexpectedly rewarding in the detection of basilar skull fracture and is certainly more available to most equine clinicians. Early detection of a basilar skull fracture is vital in providing prognosis, as horses diagnosed with such fractures are 7.5 times less likely to survive compared with those without such fractures (Feary *et al.* 2007). In our opinion, survey lateral and ventrodorsal radiography of the skull should be performed as soon as possible in horses with suspected basilar fractures. When available, CT is indicated if radiographic findings are equivocal, if the findings are incompatible with neurological deficit manifestation or if surgical intervention is intended.

Acknowledgements

The authors would like to thank Sr Beverly Olivier for her kind assistance in radiography and CT and Dr Jeanne de Villiers for referring this case to the Onderstepoort Veterinary Academic Hospital.

Competing interests

The authors declare that they have no financial or personal relationship(s) that may have inappropriately influenced them in writing this article.

Authors' contributions

C.K.L. (University of Pretoria) is the primary author and was responsible for interpretation of the CT and radiographic images as well as writing of the manuscript and final proofreading. M.N.S. (University of Pretoria) and A.V. (University of Pretoria) were the primary clinicians for this case and provided intellectual input to the manuscript. A.C. (University of Pretoria) assisted in the radiographic interpretation, provided valuable input to the manuscript and assisted in the final proofreading of the manuscript.

References

Ackerman, N., Coffman, J.R. & Corley, E.A., 1974, 'The spheno-occipital suture of the horse: Its normal radiographic appearance', *American Veterinary Radiology Society* 15, 79–81.

Avella, C.S. & Perkins, J.D., 2011, 'Computed tomography in the investigation of trauma to the ventral cranium', *Equine Veterinary Education* 23, 333–338. http://dx.doi.org/10.1111/j.2042-3292.2011.00253.x

Beccati, F., Angeli, G., Secco, I., Contini, A., Gialletti, R. & Pepe, M., 2011, 'Comminuted basilar skull fracture in a colt: Use of computed tomography to aid the diagnosis', *Equine Veterinary Education* 23, 327–332. http://dx.doi.org/10.1111/j.2042-3292.2010.00158.x

Butler, J.A., Colles, C.M., Dyson, S.J., Kold, S.E. & Poulos, P.W., 2008, 'The head', in J.A. Butler, C.M. Colles, S.J. Dyson, S.E. Kold & P.W. Poulos (eds.), *Clinical radiology of the horse,* 3rd edn., pp. 413–503, Wiley-Blackwell, Ames.

Feary, D.J., Magdesian, K.G., Aleman, M.A. & Rhodes, D.M., 2007, 'Traumatic brain injury in horses: 34 cases (1994–2004)', *Journal of the American Veterinary Medical Association* 231, 259–266. http://dx.doi.org/10.2460/javma.231.2.259, PMid:17630894

Feige, K., Furst, A., Kaser-Hotz, B. & Ossent, P., 2000, 'Traumatic injury to the central nervous system in horses: Occurrence, diagnosis and outcome', *Equine Veterinary Education* 12, 220–224. http://dx.doi.org/10.1111/j.2042-3292.2000.tb00044.x

Fiirgaard, B. & Madsen, F.H., 1997, 'Spinal epidural lipomatosis. Case report and review of the literature', *Scandinavian Journal of Medicine and Science in Sports* 7, 354–357. http://dx.doi.org/10.1111/j.1600-0838.1997.tb00166.x, PMid:9458502

Jose-Cunilleras, E. & Piercy, R.J., 2007, 'Advanced diagnostic imaging options in horses with neurological disease that localises to the head', *Equine Veterinary Education* 19, 179–181. http://dx.doi.org/10.2746/095777307X196892

Kinns, J. & Pease, A., 2009, 'Computed tomography in the evaluation of the equine head', *Equine Veterinary Education* 21, 291–294. http://dx.doi.org/10.2746/095777309X423022

Lacombe, V.A., Sogaro-Robinson, C. & Reed, S.M., 2010, 'Diagnostic utility of computed tomography imaging in equine intracranial conditions', *Equine Veterinary Journal* 42, 393–399. http://dx.doi.org/10.1111/j.2042-3306.2010.00086.x, PMid:20636774

McSloy, A.C., Forrest, L., Steinberg, H. & Semrad, S., 2007, 'Basilar skull fracture evaluated via computed tomography', *Compendium: Equine Edition* 2, 40–46.

Morrow, K.L., Park, R.D., Spurgeon, T.L., Stashak, T.S. & Arceneaux, B., 2000, 'Computed tomographic imaging of the equine head', *Veterinary Radiology and Ultrasound* 41, 491–497. http://dx.doi.org/10.1111/j.1740-8261.2000.tb01876.x, PMid:11130787

Pollard, R.E., Pulchalski, S.M. & Pascoe, P.J., 2008, 'Hemodynamic and serum biochemical alterations associated with intravenous administration of three types of contrast media in anesthetized dogs', *American Journal of Veterinary Research* 69, 1268–1273. http://dx.doi.org/10.2460/ajvr.69.10.1268, PMid:18828681

Ragle, C.A., 1993, 'Head trauma', *Veterinary Clinics of North America: Equine Practice* 9, 171–183. PMid:8472199

Ragle, C.A., Koblik, P.D., Pascoe, J.R. & Honnas, C.M., 1988, 'Computed tomographic evaluation of head trauma in a foal', *Veterinary Radiology* 29, 206–208. http://dx.doi.org/10.1111/j.1740-8261.1988.tb01500.x

Ramirez III, O., Jorgensen, J.S. & Thrall, D.E., 1998, 'Imaging basilar skull fractures in the horse: A review', *Veterinary Radiology and Ultrasound* 39, 391–395. http://dx.doi.org/10.1111/j.1740-8261.1998.tb01624.x, PMid:9771589

Seiler, G., Kinns, J., Dennison, S., Saunders, J. & Schwarz, T., 2011, 'Vertebral column and spinal cord', in T. Schwarz & J. Saunders (eds.), *Veterinary computed tomography,* pp. 209–228, Wiley-Blackwell, Chichester.

Sogaro-Robinson, C., Lacombe, V.A, Reed, S.M. & Balkrishnan, R., 2009, 'Factors predictive of abnormal results for computed tomography of the head in horses affected by neurologic disorders: 57 cases (2001–2007)', *Journal of the American Veterinary Medical Association* 235, 176–183. http://dx.doi.org/10.2460/javma.235.2.176, PMid:19601739

Solano, M. & Brawer, R.S., 2004, 'CT of the equine head: Technical considerations, anatomic guide, and selected diseases', *Clinical Techniques in Equine Practice* 3, 374–388. http://dx.doi.org/10.1053/j.ctep.2005.02.016

Taylor, D.S., Wisner, E.R., Kuesis, B.S., Smith, S.G. & O'Brien, T.R., 1993, 'Gas accumulation in the subarachnoid space resulting from blunt trauma to the occipital region of a horse', *Veterinary Radiology and Ultrasound* 34, 191–193. http://dx.doi.org/10.1111/j.1740-8261.1993.tb02004.x